Hydroperiod regime controls the organization of plant species in wetlands

Romano Foti[a], Manuel del Jesus[a,b], Andrea Rinaldo[c,d], and Ignacio Rodriguez-Iturbe[a,1]

[a]Department of Civil and Environmental Engineering, Princeton University, Princeton, NJ 08544; [b]Environmental Hydraulics Institute "Instituto de Hidraulica de Cantabria," Universidad de Cantabria, 39005 Santander, Spain; [c]Dipartimento di Ingegneria Idraulica Marittima Ambientale e Geotecnica and Centro Internazionale di Idrologia "Dino Tonini," Università di Padova, I-35131 Padova, Italy; and [d]Laboratory of Ecohydrology, Faculté Environnement Naturel, Architectural et Construit, École Polytechnique Fédérale, CH-1015 Lausanne, Switzerland

Contributed by Ignacio Rodriguez-Iturbe, October 17, 2012 (sent for review July 24, 2012)

With urban, agricultural, and industrial needs growing throughout the past decades, wetland ecosystems have experienced profound changes. Most critically, the biodiversity of wetlands is intimately linked to its hydrologic dynamics, which in turn are being drastically altered by ongoing climate changes. Hydroperiod regimes, e.g., percentage of time a site is inundated, exert critical control in the creation of niches for different plant species in wetlands. However, the spatial signatures of the organization of plant species in wetlands and how the different drivers interact to yield such signatures are unknown. Focusing on Everglades National Park (ENP) in Florida, we show here that cluster sizes of each species follow a power law probability distribution and that such clusters have well-defined fractal characteristics. Moreover, we individuate and model those signatures via the interplay between global forcings arising from the hydroperiod regime and local controls exerted by neighboring vegetation. With power law clustering often associated with systems near critical transitions, our findings are highly relevant for the management of wetland ecosystems. In addition, our results show that changes in climate and land management have a quantifiable predictable impact on the type of vegetation and its spatial organization in wetlands.

ecology | self-organization | ecosystems sensitivity | wetlands vulnerability

With the richness and complexity of their ecosystems, wetland areas are of growing interest as they host a variety of animal and vegetal species, many of which are rare or endangered, and constitute some of the most unique and beautiful areas in the world. Once perceived simply as worthless swamps, wetlands have been subjected to a great deal of degradation throughout the past decades, as more and more of their land has been seized and reconverted to suit the needs of the growing human population (1, 2). Today, their value is being rediscovered and the preservation of their ecosystem and biodiversity is acquiring major importance. Under this perspective, understanding the dynamics that control the delicate equilibrium of wetland ecosystems is vitally important, as it is the key to develop both preservation and restoration measures. Given that ecosystems can abruptly shift from an existing state to another in response to changes in the system forcings (3–6), a quantitative analysis of wetlands dynamics is a timely issue, especially in scenarios that may be complicated by ongoing and future climatic changes (7–9).

Vegetation patterns are frequently the result of the interplay between local dynamics and global forcings (10, 11) and thus can be described by the interaction between these drivers (10–16). However, given the typical complexity of wetland ecosystems and the heterogeneity of their hydrologic regimes, isolating key global drivers as well as determining the strength and range of the local dynamics is a challenging task. The number of factors that affect the spatial distribution of plant species in wetlands is in fact quite large, as they include a large number of local and global dynamics that control their hydrologic and thermodynamic regime.

Results

Spatial Analysis of Everglades National Park. We begin by examining the spatial distribution of vegetation types across the freshwater portion of Everglades National Park (ENP) in Florida and investigate the impact of the main hydrologic drivers on the structure of the vegetative communities. Whereas the ecosystem of ENP is extremely diverse and hosts a large variety of vegetal and animal species across a wide range of topographic and hydrologic conditions, its landscape is widely dominated by thick, razor-edged sawgrass (*Claudium jamaicense*), which covers over 60% of its surface (7, 17). The attempt to link hydropatterns to the spatial structure of the various vegetation communities of ENP has been the focus of many studies and the segregation of certain species within particular hydrologic niches has been widely observed (17–21). Species as, for example, muhly grass (*Muhlenbergia filipes*) predominantly colonize rarely flooded areas, whereas red mangrove shrub (*Rhizophora mangle*) is most commonly found in frequently flooded ones (17). The overall spatial structuring of ENP, however, cannot be explained accounting for only hydrologic drivers, while neglecting the critical role of the interactions among species and between vegetation with the environment (14, 22). Here we describe ENP vegetation pattern dynamics via interactions between exogenous, globally driven forces (i.e., hydropatterns) and local, endogenous processes of facilitation–competition.

We determine the spatial distribution of the different plant species across ENP through the 1:15,000 scale mapping and classification of its 79 plant communities (23, 24). We adopt a 40×40 m grid to extract the dominant vegetation type at each location. Concurrently, we use the hydrologic information provided by the Everglades Depth Estimation Network (EDEN) to produce a 40×40 m grid of the percentage of time each location is inundated (PTI) (25, 26). A complete description of the vegetation and hydrologic datasets are provided in *SI Text*. Among all of the plant species present in ENP, we selected for the study those 13 that individually cover at least 1% of its area. A map of the average PTI across ENP is provided in Fig. 1. As shown also in Fig. 1, PTI conditions provide niches of colonization for different types of vegetation: tall sawgrass prevails in frequently flooded areas, whereas pine savanna (*Pinus elliottii* var. *densa*) occurs prevalently where hydroperiods are less likely to occur. On the other hand, sawgrass is found with similar prevalence across almost all PTI conditions (with the notable exception of very low PTI values), a characteristic that is unique among all of the types analyzed. In addition to the vegetation density, estimated as the fraction of pixels occupied by each vegetation species, we calculated the vegetation pair density as the fraction of adjacent pixels occupied by the same vegetation type (27). For all species, the value of the pair density is found to be close to that of the vegetation density

Author contributions: R.F., M.d.J., and I.R.-I. designed research; R.F. performed research; R.F., M.d.J., A.R., and I.R.-I. analyzed data; and R.F., M.d.J., A.R., and I.R.-I. wrote the paper.

The authors declare no conflict of interest.

Freely available online through the PNAS open access option.

[1]To whom correspondence should be addressed. E-mail: irodrigu@princeton.edu.

This article contains supporting information online at www.pnas.org/lookup/suppl/doi:10.1073/pnas.1218056109/-/DCSupplemental.

Downloaded by guest on June 12, 2021

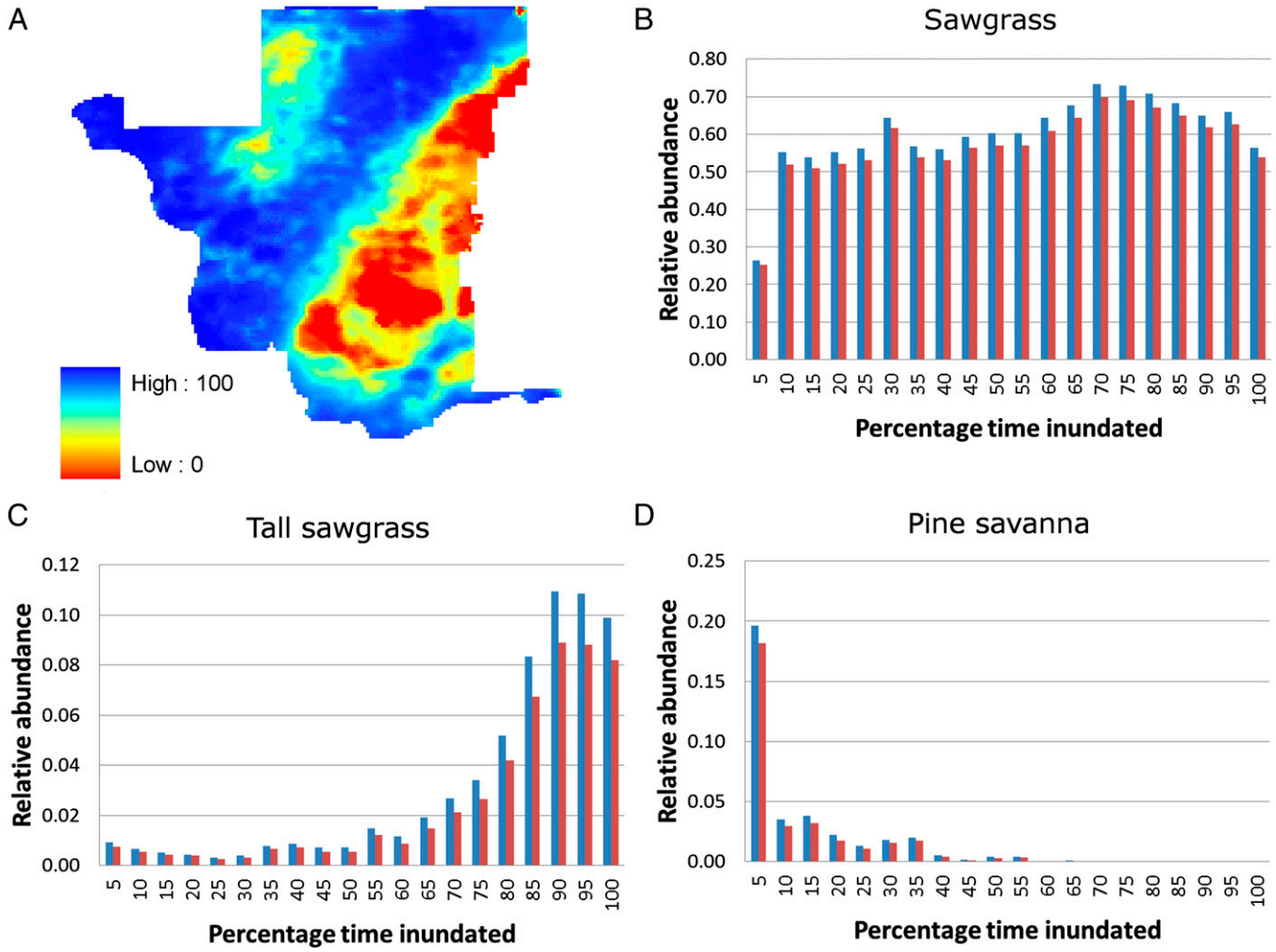

Fig. 1. Hydroperiod regimes provide niches for vegetation species. (*A*) Map of the average percentage time inundated across ENP. Vegetation density (blue bars) and pair vegetation density (red bars) versus percentage time inundated for (*B*) sawgrass, (*C*) tall sawgrass, and (*D*) pine savanna.

across all PTIs, suggesting that plants of the same species tend to be found in clumps rather than being randomly dispersed in space with a certain overall density. In addition to their density and pair density, we analyze the spatial structure of each of those 13 species through the probability that the area of a cluster, A, is greater or equal to a certain value a, $P(A \geq a)$. For each species considered, a cluster is made up of pixels that share any of their four edges at the 40×40 m scale grid. Interestingly, the cluster size of all of the selected types are distributed according to power laws, $P(A \geq a)\ \alpha\ a^{-\beta}$, over a span of three or more orders of magnitude. We analyze the fractal characteristics of the spatial structures of individual species through the cluster's perimeter–area relationship as well as the box-counting fractal dimension. The cluster size distributions, the cluster area–perimeter relationships, and the box-counting fractal dimensions for sawgrass, tall sawgrass, and pine savanna are shown in Fig. 2 and Table 1 (see *SI Text* for a complete description of the 13 species).

The implications of power law distributed cluster sizes, as well as the fractal structure of clusters are noteworthy. The existence of power laws in natural systems is often associated with self-organization (28–31) and dynamics occurring near critical transition points (15, 32). Although the presence of power laws per se does not imply that the system is indeed at a phase transition critical state (11, 14, 33, 34), their occurrence in an ecosystem that is open, dissipative, and with many degrees of freedom, such as ENP, merits close examination.

Modeling of the Vegetation Dynamics. To capture the key drivers of the spatial structuring of the vegetation communities within ENP, we simulate the system via a multistate cellular automaton model. For all simulations, we adopt the same 40×40 m grid overlaying ENP, thus facilitating comparisons between simulated results and observations. Starting with an initial random spatial distribution of the 13 selected species, we simulate the system by assigning to each cell a probability of transition between one state (i.e., one plant species) and another.

To do so, we developed a 14-state cellular automaton model, each state corresponding to the 13 most frequent vegetation species, and a null state representing all of the other species. Transition probabilities between states reflect the influence of both the global driver (PTI) and the local feedback dynamics, such as facilitation/competition for available resources, seed dispersal, and germination (10, 11, 14). The model has only one arbitrary parameter, which represents the rate of decay of the local feedback in the neighborhood of each cell (*Methods*).

Several simulations were carried out by using different weighting schemes (exponential or Pareto) and by varying the rate of decay (represented by the arbitrary parameter k). The model was particularly robust in replicating all of the key spatial statistics regardless of the weighting scheme or the specific value of the parameter.

The model is capable of replicating the observed spatial statistics, namely, the density and pair density for each species, as

Downloaded by guest on June 12, 2021

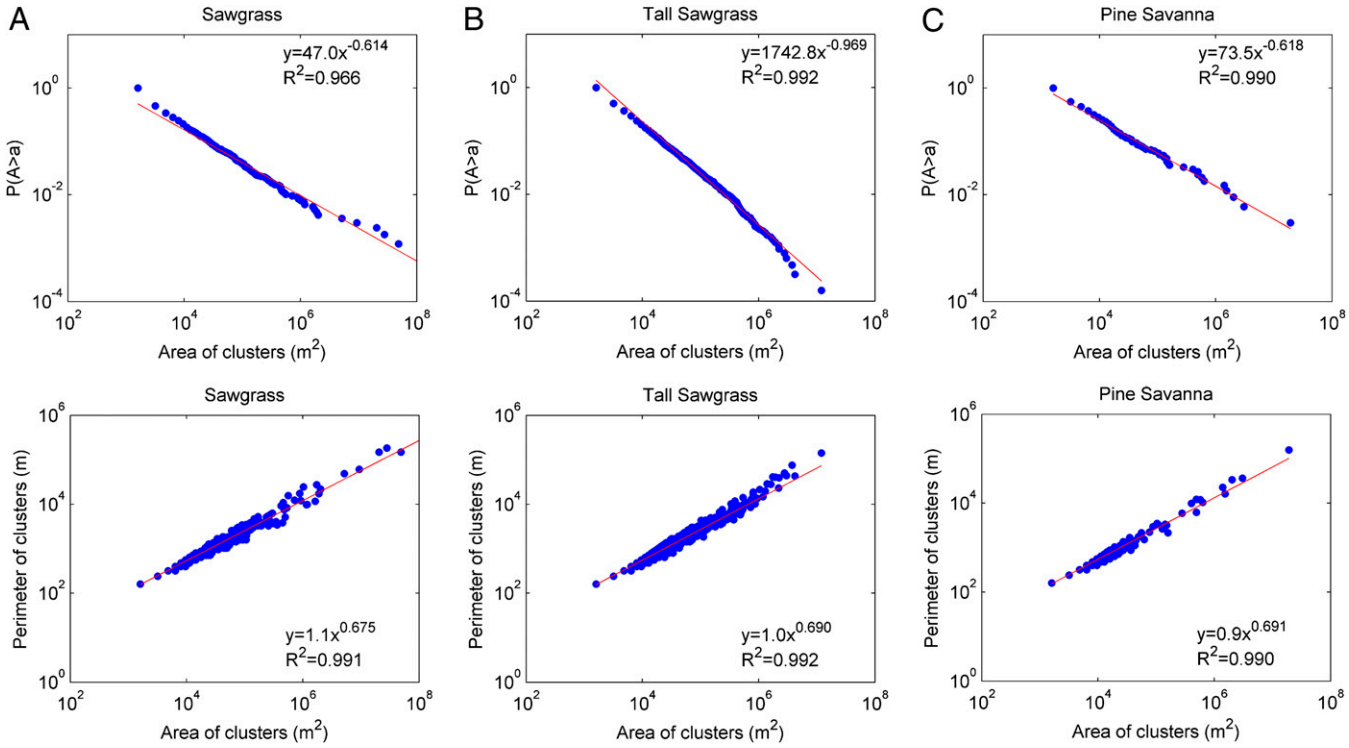

Fig. 2. Observed cluster size distribution and perimeter–area relationships for (*A*) sawgrass, (*B*) tall sawgrass, and (*C*) pine savanna.

well as the clustering patterns of individual species communities, namely, the power law distribution of the cluster size, the perimeter–area fractal structure, and the box-counting fractal dimension. Although there are some expected differences in the numerical values between observed and simulated patterns, their overall similarity is remarkable. Results for sawgrass, tall sawgrass, and pine savanna are reported in Table 1 and Fig. 3, whereas full results for all species are given in *SI Text*.

Discussion and Conclusions

Remarkably, the reproduction of the spatial organization is achieved with no fine tuning of the model-only parameter. In addition, matching observations of relative abundance, pair density, and cluster size distributions for the plant species of ENP is only achieved when both global controls and local interactions are implemented in the model. We conclude that the spatial structure of the vegetation communities is indeed driven by the environmental hydropatterns (i.e., hydroperiod regimes) and local short-range feedback. We also suggest that the relative abundance of species is crucially dependent on the hydroperiods as well as on the fact that the power law behavior of species cluster size distributions is observed throughout the whole domain, despite the fact that the exogenous forcing (i.e., PTI) is not globally applied and exerts site-specific control on vegetation.

The ubiquity of the scaling features of power laws, reproduced by the cellular automaton across species and hydropatterns, suggests that the ENP ecosystem is in a self-organized critical state (29) where no characteristic cluster size exists. The sensitivity of the system to perturbations, both in terms of species prevalence and in terms of patterning and cluster size distribution is the object of our ongoing research. Nevertheless, the embedded robustness of the dynamic origins of the patterns found within ENP has important implications. The hydrologic regime of wetlands is, in fact, extremely sensitive to changes in both precipitation and evapotranspiration patterns as well as to anthropic activity resulting in hydroperiod regime shifts. Our results suggest that changes in climate and land management have a strong and quantifiable predictable impact on vegetation patterns and species distribution.

Methods

A 14-state cellular automaton model was developed to simulate ENP, each state corresponding to the 13 most frequent vegetation species and to a null state representing all of the other species. Transition probabilities between states reflect the influence of both the global driver (PTI) and the local feedback dynamics (6).

Starting with a random spatial distribution of the 14 states, the domain is updated according to the following steps:

1) A pixel is chosen at random.

Table 1. Observed and modeled spatial statistics of plant species within ENP

	Observed					Modeled				
	ρ_0	ρ_{00}	β	γ	D_B	ρ_0	ρ_{00}	β	γ	D_B
Sawgrass	0.606	0.587	−0.614 [−0.636–0.592]	0.675 [0.672–0.679]	1.76	0.605	0.534	−0.817 [−0.852–0.783]	0.670 [0.669 0.672]	1.78
Tall sawgrass	0.058	0.048	−0.969 [−0.982–0.957]	0.690 [0.688–0.691]	1.46	0.057	0.039	−0.956 [−0.969–0.943]	0.684 [0.683 0.686]	1.46
Pine savanna	0.016	0.014	−0.618 [−0.636–0.599]	0.690 [0.684–0.699]	1.31	0.017	0.011	−0.777 [−0.805–0.749]	0.654 [0.652 0.657]	1.26

Statistics of vegetation density (ρ_0), vegetation pair density (ρ_{00}), slope of the cluster size distribution (β) with 95% confidence intervals, slope of the cluster perimeter-area relationship (γ) with 95% confidence intervals, and box-counting fractal dimension (D_B) for selected vegetation species.

Downloaded by guest on June 12, 2021

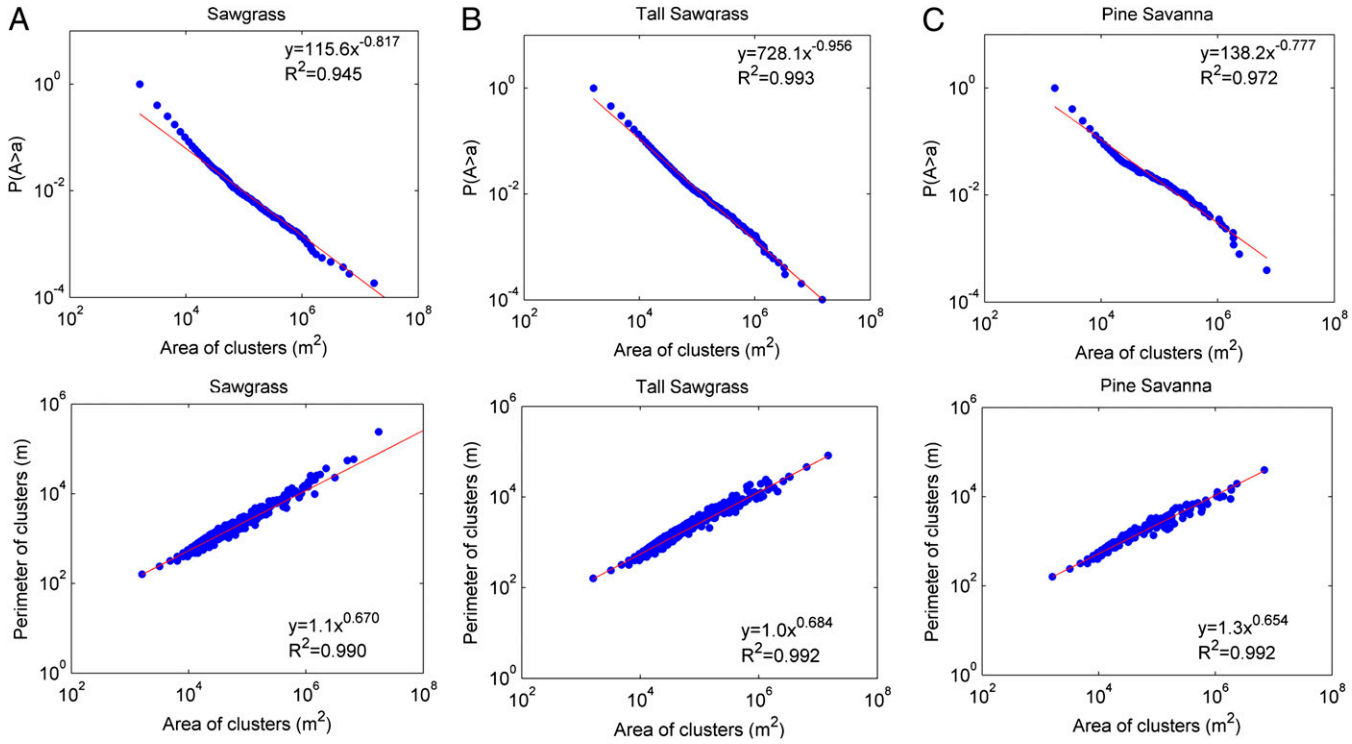

Fig. 3. Modeled cluster size distribution and perimeter–area relationships for (*A*) sawgrass, (*B*) tall sawgrass, and (*C*) pine savanna.

2) The probability of transitioning from the current vegetation species present at that pixel to a new one is evaluated as follows:

$$P\left(V_i \to \overline{V_i}\right) = \left(1 - r^{(i)}\right) + \left(\rho_{0_M}^{(i)} - \rho_{0_T}^{(i)}\right) \Big/ \rho_{0_M}^{(i)},$$

where:

$\rho_{0_M}^{(i)}$ is the density of species V_i measured at the given iteration for the subdomain defined by the PTI bin to which the given pixel belongs.

$\rho_{0_T}^{(i)}$ is the target density of species V_i, as estimated from a polynomial fit of the observed vegetation density of species V_i, across PTI bins.

r is the effect of the local feedback, estimated as follows:

$$r^{(i)} = \frac{\sum_j \exp(-kd_{ij})v_j}{\sum_j \exp(-kd_{ij})}$$

for exponential decay of the lateral interactions, or

$$r^{(i)} = \frac{\sum_i \left(\frac{1}{d_{ij}}\right)^k v_j}{\sum_j \left(\frac{1}{d_{ij}}\right)^k}$$

for Pareto weighting scheme of the lateral interactions. In the previous equations, d_{ij} represents the distance between pixel j and pixel i (where the species V_i is located), v_j is equal to 1 if the vegetation cell of pixel j is the same as V_i and 0 otherwise, and k is an arbitrary parameter that represents the spatial decay of the strength of interaction. The sum is evaluated over all of the closest neighbors such that the cumulative function would exceed 0.95.

3) If the transition occurs, each of the other states will be selected with a probability given by:

$$P\left(\overline{V_i} \to V_l\right) = \frac{r^{(l)} + \left(\rho_{0_M}^{(l)} - \rho_{0_T}^{(l)}\right) \Big/ \left(1 - \rho_{0_M}^{(l)}\right)}{\Omega},$$

where Ω is a normalizing constant that ensures that the sum of the probabilities of transition from state i to any other state equals one:

$$\Omega = \sum_{n=1, n \neq i}^{14} r^{(n)} + \left(\rho_{0_M}^{(n)} - \rho_{0_T}^{(n)}\right) \Big/ \left(1 - \rho_{0_M}^{(n)}\right).$$

A flowchart of the modeling procedure is provided in *Supporting Information*.

The total number of iterations (i.e., the total number of times a pixel is chosen for transition to another vegetation state) is set to be 120 million. Given the domain size and the spatial resolution, this implies that each pixel is selected for update an average of 90 times, which was observed to be enough for the spatial statistics to stabilize. A sample set of snapshots of the modeled system relative to sawgrass is provided in *Supporting Information*.

ACKNOWLEDGMENTS. We thank Jason M. Todd for assistance with the hydrologic and vegetation datasets. This research has been funded by National Aeronautics and Space Administration (NASA)'s Science of Coupled Aquatic Processes in Ecosystems from Space (WaterSCAPES) (NASA NNX08BA43A).

1. Grunwald M (2006) *The Swamp* (Simon & Schuster, New York).
2. Sklar FH, et al. (2005) The ecological-societal underpinnings of Everglades restoration. *Front Ecol Environ* (3):161–169.
3. Barnosky AD, et al. (2012) Approaching a state shift in Earth's biosphere. *Nature* 486 (7401):52–58.
4. Scheffer M, et al. (2009) Early-warning signals for critical transitions. *Nature* 461 (7260):53–59.
5. Drake JM, Griffen BD (2010) Early warning signals of extinction in deteriorating environments. *Nature* 467(7314):456–459.
6. Scheffer M, Carpenter S, Foley JA, Folke C, Walker B (2001) Catastrophic shifts in ecosystems. *Nature* 413(6856):591–596.
7. Todd MJ, Muneepeerakul R, Miralles-Wlhelm F, Rinaldo A, Rodriguez-Iturbe I (2012) Possible climate change impacts on the hydrological and vegetation character of Everglades National Park, Florida. *Ecohydrology* 5:326–336.
8. Bernhardt CE, Willard DA (2009) Response of the Everglades ridge and slough landscape to climate variability and 20th-century water management. *Ecol Appl* 19(7): 1723–1738.
9. Pearlstine LG (2009) Potential ecological consequences of climate change in South Florida and the Everglades: 2008 literature synthesis, in *South Florida Natural Resouces Center Technical Series* (National Park Service, US Department of the Interior, Homestead, FL).
10. Kéfi S, et al. (2007) Spatial vegetation patterns and imminent desertification in Mediterranean arid ecosystems. *Nature* 449(7159):213–217.

Downloaded by guest on June 12, 2021

11. Scanlon TM, Caylor KK, Levin SA, Rodriguez-Iturbe I (2007) Positive feedbacks promote power-law clustering of Kalahari vegetation. *Nature* 449(7159):209–212.
12. Wolfram S (1984) Cellular automata as models of complexity. *Nature* 311:419–424.
13. Wootton JT (2001) Local interactions predict large-scale pattern in empirically derived cellular automata. *Nature* 413(6858):841–844.
14. Scanlon T, Caylor KK, Levin SA, Rodriguez-Iturbe I (2007) Positive feedbacks promote power-law clustering of Kalahari vegetation. *Nature* 449:209–212.
15. Solè RV, Manrubia SC (1995) Are rainforests self-organized in a critical state? *J Theor Biol* 173:31–40.
16. Callaway RM, Walker LR (1997) Competition and facilitation: A synthetic approach to interactions in plant communities. *Ecology* 78:1958–1965.
17. Todd MJ, et al. (2010) Hydrological drivers of wetland vegetation community distribution within Everglades National Park, Florida. *Adv Water Resour* 33:1279–1289.
18. Davis SM, Gunderson LH, Park WW, Richardson JR, Mattson JE (1994) Landscape dimension, composition and function in a changing Everglades ecosystem. *Everglades: The Ecosystem and Its Restoration* (St. Lucie Press, Delray Beach, FL).
19. Ross MS, Reed DL, Sah JP, Ruiz PL, Lewin MT (2003) Vegetation:environment relationships and water management in Shark Slough, Everglades National Park. *Wetlands Ecol Manage* 11:291–303.
20. Zweig CL, Kitchens WM (2008) Effects of landscape gradients on wetland vegetation communities: Information for large-scale restoration. *Wetlands* 28(4):1086–1096.
21. Armentano TV, et al. (2006) Rapid responses of vegetation to hydrological changes in Taylor Slough, Everglades National Park, Florida, USA. *Hydrobiologia* 569:293–309.
22. Marani M, Zillio T, Belluco E, Silvestri S, Maritan A (2006) Non-neutral vegetation dynamics. *PLoS ONE* 1(1):e78.
23. Welch R, Madden M, Doren R (2001) Vegetation map and digital database of South Florida's National Park Lands. *The Everglades, Florida Bay, and Coral Reefs of the Florida Keys: An Ecosystem Sourcebook* (CRC, Boca Raton, FL).
24. Welch R, Madden M (1999) Mapping of the Everglades. *Photogramm Eng Remote Sensing* 65(2):163–170.
25. Conrads PA, Roehl EA (2007) *Hydrologic Record Extension of Water-Level Data in the Everglades Depth Estimation Network (EDEN) using Artificial Neural Network Models, 2000-2006*, US Geological Survey Open-File Report 2007-1350. Available at: http://pubs.water.usgs.gov/ofr2007–1350).
26. Telis PA (2006) The Everglades Depth Estimation Network (EDEN) for Support of Ecological and Biological Assessments. U.S. Geological Survey Fact Sheet 2006-3087 (USGS, Reston, VA).
27. Kizaki S, Katori M (1999) Analysis of canopy-gap structures of forests by Ising-Gibbs states: Equilibrium and scaling property of real forests. *J Phys Soc Jpn* 68:2553–2560.
28. Pascual M, Roy M, Guichard F, Flierl G (2002) Cluster size distributions: Signatures of self-organization in spatial ecologies. *Philos Trans R Soc Lond B Biol Sci* 357(1421): 657–666.
29. Bak P, Tang C, Wiesenfeld K (1987) Self-organized criticality: An explanation of the 1/f noise. *Phys Rev Lett* 59(4):381–384.
30. Brown JH, et al. (2002) The fractal nature of nature: Power laws, ecological complexity and biodiversity. *Philos Trans R Soc Lond B Biol Sci* 357(1421):619–626.
31. Malamud BD, Morein G, Turcotte DL (1998) Forest fires: An example of self-organized critical behavior. *Science* 281(5384):1840–1842.
32. Yeomans JM (1992) *Statistical Mechanics of Phase Transitions* (Oxford Univ Press, London).
33. Pascual M, Guichard F (2005) Criticality and disturbance in spatial ecological systems. *Trends Ecol Evol* 20(2):88–95.
34. Marani M, Lanzoni S, Silvestri S, Rinaldo A (2004) Tidal landforms, patterns of halophytic vegetation and the fate of the lagoon of Venice. *J Mar Syst* 51:191–210.

Downloaded by guest on June 12, 2021